IEEE*Access*

Multidisciplinary : Rapid Review : Open Access Journal

Near-Optimal PI Controllers of STATCOM for Efficient Hybrid Renewable Power System

MOHAMED I. MOSAAD[1], **HAITHAM SAAD MOHAMED RAMADAN**[2,3],
MANSOUR ALJOHANI[1], **MOHAMED F. EL-NAGGAR**[4,5],
AND SHERIF S. M. GHONEIM[6], **(Senior Member, IEEE)**

[1]Yanbu Industrial College (YIC), Yanbu 46452, Saudi Arabia
[2]ISTHY, l'Institut International sur le Stockage de l'Hydrogène, 90400 Meroux-Moval, France
[3]Electrical Power and Machines Department, Faculty of Engineering, Zagazig University, Zagazig 44519, Egypt
[4]Department of Electrical Engineering, College of Engineering, Prince Sattam Bin Abdulaziz University, Al-Kharj 16273, Saudi Arabia
[5]Department of Electrical Power and Machines Engineering, Faculty of Engineering, Helwan University, Helwan 11795, Egypt
[6]Electrical Engineering Department, College of Engineering, Taif University, Taif 21944, Saudi Arabia

Corresponding author: Mohamed I. Mosaad (m_i_mosaad@hotmail.com) and Haitham Saad Mohamed Ramadan
(haitham.mohamed-ramadan@utbm.fr)

ABSTRACT Connecting different renewable energy sources (RESs) to the electrical grids is presently being urged to fulfill the enormous need for electric power and to decrease traditional sources' ecological related issues, the so-called hybrid systems. Unfortunately, these hybrid systems suffer from the possible negative environmental impacts of the wind gusts in wind energy conversion systems (WECSs) that may degrade the overall system performance. Additionally, various severe faults may disconnect some RESs from the hybrid system, like three-phase faults. In this paper, the static synchronous compensator (STATCOM) is considered for both improving the performance of a hybrid system, contains WECS and photovoltaics (PVs) against wind gusts and maintaining the continuous operations of RESs during three-phase fault occur at the point of common coupling (PCC) between the RESs and the grid. The STATCOM is stimulated by two PI controllers regulating the reactive power flow between the STATCOM and the hybrid system at PCC and, consequently, regulating the voltage at PCC. A metaheuristic optimizer optimally schedules these two PI controllers based on whale optimization algorithm (WOA). The impartial comparison between the WOA dynamic performance and the particle swarm optimization as another optimization algorithm verifies the efficiency of the WOA for the near-optimal gain scheduling of the PI controller gains.

INDEX TERMS Renewable energy, hybrid power systems, wind energy, PV, STATCOM, PI controller, reactive power regulation, Whale optimization algorithm.

ABBREVIATIONS

a	Diode constant of ideality.
AVR	Automatic voltage regulator
ANN	Artificial neural network
ANFIS	Adaptive-Network-Based Fuzzy Inference System
CSO	Cuckoo search optimization
DFIG	Doubly-fed induction generator
DVR	Dynamic Voltage Restorer
ev	Error between the PCC and reference voltages
FACTS	Flexible AC Transmission systems
FC	Fuel cell
G	Instantaneous irradiance

G_n	Irradiance at nominal conditions
GA	Genetic algorithm
I_m	Module current.
I_{scn}	PV short circuit current
I_o	Reverse leakage current of the diode
I_{pv}	PV current.
I_{pvn}	PV current at generated at 25 °C and 1000 W/m^2.
K	Boltzmann constant
K_v	Voltage temperature coefficient
N_s	Number of series PV modules
N_p	Number of parallel PV modules
Nsg	Phases number of SRG
PCC	Point of common coupling
PI	Proportional Integral
PSO	Particle swarm optimization

The associate editor coordinating the review of this manuscript and approving it for publication was Sanjeevikumar Padmanaban.

|	
PV	Photovoltaic
RESs	Renewable energy sources
R_s	Series resistances of PV module
Rsg	SRG stator resistance
R_p	Parallel resistances of PV module
q	Electron charge
SEIG	Self-excited induction generator
SRG	Switched-reluctance generator
SSSC	Static synchronous series compensator
STATCOM	Static synchronous compensators
SVC	Static VAR compensator
T	P-N junction temperature in Kelvin
T_G	Conduction period of one phase
UPFC	Unified power flow controller
V_{ocn}	PV open circuit voltage
VSD	Voltage source converter
WOA	Whale optimization algorithm
WECS	Wind energy conversion system
α	Turn-on angles of each phase
μ	Turn-off angles of each phase
ΔT	Difference between the actual and the nominal temperature
$\overrightarrow{Y}$	Position vector for the current obtained best solution
$\overrightarrow{Y^P}$	Best prey position vector
F'	Finest location between whale and prey
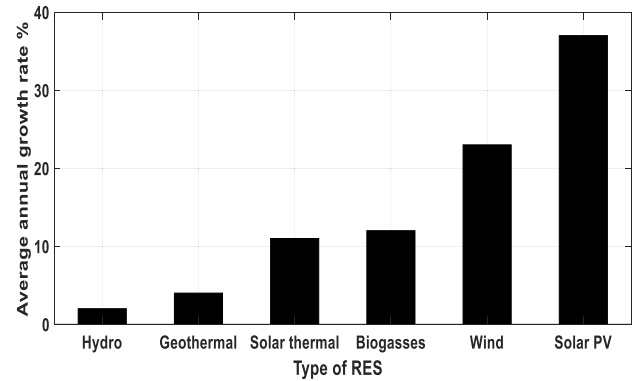
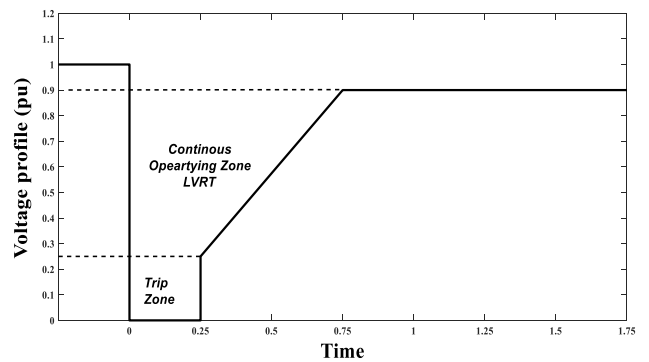**FIGURE 1. Annual growth rate of some RESs.**

FIGURE 2. Nordal grid code.

I. INTRODUCTION

The integration of renewable energy sources (RESs) into electrical systems has become a necessary and essential matter to face the large increase in electrical energy demand and reduce pollution problemscaused by using fossil fuels. Different types of RESs are used in generating electric power, including wind, photovoltaic (PV), Fuel cell, and biomass [1]–[4]. The two most RESs integrated into the electrical systems are the wind and the PV in favor of their multiple advantages, which is evident from the annual growth rate of RESs, Fig. 1, [5].

Hybrid power systems based on wind energy conversion systems (WECSs) and PV systems cannot supply the required reactive power during fault events in the system. Consequently, the voltage profile at the point of common coupling (PCC) between the RESs and the grid will fluctuate. These voltage fluctuations have adverse effects on the power system performance, including system stability, power factor and power quality. Moreover, if not properly controlled, these voltage fluctuations will range to undesirable levels that will lead to the disconnection of these RESs from the system due to the lack of supporting the system's reactive power during these faults according to some grid codes, Nordal grid code as an example is shown in Fig.2, [6].

The improper control of voltage fluctuations results in undesired disconnection of RESs from the system because of the lack of supporting the system's reactive power during

these faults according to some grid codes Nordal grid code as an example is shown in Fig.2 [6].

Various types of electrical generators were utilized in WECSs, such as self-excited induction generators (SEIGs), doubly-fed induction generators (DFIGs) and switched reluctance generators (SRGs). Despite the simple construction of the SEIGs, they are sensitive to wind speed variations and cannot operate wide speed ranges [7]. DFIGs are not sensitive to wind speed variations and can operate at wide speed ranges. However, DFIGs have high faulty sensitivity and need continuous maintenance due to the rotor slip-ring structure [8]. Owing to their advantages, SRGs are commonly used in many WECS applications. Their cheapness, robustness andlack of continuous maintenance are among the SRGs' particular features despite the requirement of reactive power support [9].

Reactive power support for hybrid power systems needs some external devices during faulty events, using flexible AC transmission systems (FACTS) devices [10], [11]. These devices play an essential role in improving the connection of RESs into the power system by supporting reactive power. FACTS devices can be categorized according to their connection to the system into series, shunt and series/shunt combination. Each category has its own usage and characteristics. Series FACTS devices are used for increasing the transmission line capacity and adjusting the line reactances. The series

compensators used in hybrid renewable systems, dynamic voltage restorer (DVR) are highlighted in [12]. Shunt devices support the voltage by injecting/absorbing reactive power during voltage sag/swell conditions, respectively. Shunt compensators like static VAR compensators (SVCs) and static synchronous compensators (STATCOMs) and superconductors are presented for controlling different grid-connected RESs [13], [14]. Moreover, the compound type, which is a combination of series and shunt FACTS devices, such as the unified power flow controller (UPFC), was introduced to improve the connection of RESs to the grid [15]. The compound type can play the role of series and shunt FACTS devices. Various FACTS devices' applications in improving the connection of RESs to the system are summarized in Table 1.

TABLE 1. Different applications of facts devices in RESs.

FACTS device	Applications in RESs	Ref.
DVR	Enhance the performance and support the FRT capability.	[3, 12]
	Voltage sag mitigation.	[16]
	Support low-voltage ride-through capability.	[17-18]
SVC	Support the reactive power.	[7]
	Hosting the capacity.	[19]
STATCOM	Improve the power quality.	[20]
	Voltage stability improvement.00	[21]
	Power quality support.	[22]
UPFC	Support low-voltage ride through.	[15]
	Power enhancement.	[23]

So far, the classical PI controllers are still used in many applications related to the electrical generating field owing to their simplicity and straightforwardness features. PI controllers were used for enhancing hybrid power systems' performance, including fuel cell, PV, and wind [3], [20], [22], [24]. Despite all PI controllers' features, their assigned role will not correctly or adequately perform if their parameters are not appropriately determined. The typical hybrid system structure contains different power electronic devices such as converters and inverters, RESs, and controllable devices, making these systems non-linear, complex, and uncertain. The adjustment of PI controller parameters for such non-linear, uncertain, and complex systems is challenging by conventional techniques such as linear programming [25]. This challenge paves the way for modern optimization methods to tune the PI controller parameters for reaching systems optimal operating performance. The use of PI controllers for improving the connection of STATCOM to the grid was presented in [26]–[28].

Genetic algorithm (GA), presented in [29], is considered a benchmark for optimal tuning of PI controller gains. Particle swarm optimization (PSO), besides more recent optimizers based on harmony search and follower pollination, were introduced for the optimal PI-gain scheduling for FC connected to electrical networks [24]. The three optimizers were used for the near-optimal scheduling of PI-controller

gains driving the inverter connecting fuel cell to the grid. Whale optimization algorithm (WOA), among the modern optimization techniques, was proposed in different power systems applications, such as: (i) optimal tuning of FOPI controllers for controlling static synchronous series compensator (SSSC) (ii) WOA provided more efficient results than PSO [30], (iii) optimal scheduling of PID control WOA provided better dynamic performance compared to other seven optimizers [9], [30]. Some advanced modern techniques like GA, ANN, and ANFIS were presented to control STATCOM [31], [32].

This paper presents two optimized PI controllers for STATCOM to regulate the connection of two RESs, namely WECS based-SRG and PV systems, to the electrical grid. STATCOM is integrated into RES at the PCC to handle voltage fluctuation during grid side disturbance by interchanging the reactive power flow between the STATCOM and the system. By regulating the PCC voltage, the system performance is improved. Besides, it complies with grid codes and maintains the continuous operation of RESs even under fault events. The two PI controllers used for driving STATCOM are tuned using WOA. The due qualitative and qualitative comparison and impartial analysis are introduced considering the system dynamic performance while controlled using PSO and WOA-based near-optimal PI controllers.

II. SYSTEM UNDER STUDY

The studied system consists of two RESs, SRG-WECS and PV. These two RESs are connected to the system at a common coupling bus. This common coupling bus is connected to the grid through two transformers and two transmission lines. STATCOM is connected to the system at PCC to improve the system performance, as depicted in Fig. 3. The rating of the WECS is 24.8 kW. The PV system is 100 kW and composed of 100 string; each has five series-connected modules with relevant data listed in the Appendix.

III. SYSTEM MODELING

A. SWITCHED RELUCTANCE GENERATOR

The manufacture of SRG is modest as related to other kinds of electric generators. The stator windings are concentrated type and with simple architecture. For the typical structure, diametrically opposite stator windings are series-connected, forming a two-pole field pattern. The rotor is winding-less, without magnets and with possible relative low inertia. The SRG has a doubly salient pole construction (stator and rotor are salient) excited by asymmetric bridge converter. In this study, four phases, 8/6 poles SRG with the construction given in Fig.4-a is used. Fig.4-b illustrates the converter structure of a four-phase 8/6 SRG [33], [34].

The phase currents of the SRG can be independently controlled by feeding the four-phase using an asymmetrical power converter. The rotor position is sensed. Therefore, the (turn-on and off) angles (μ and β) respectively of each phase can faultless performed. The four independent hysteresis controller is used for controlling the currents in stator

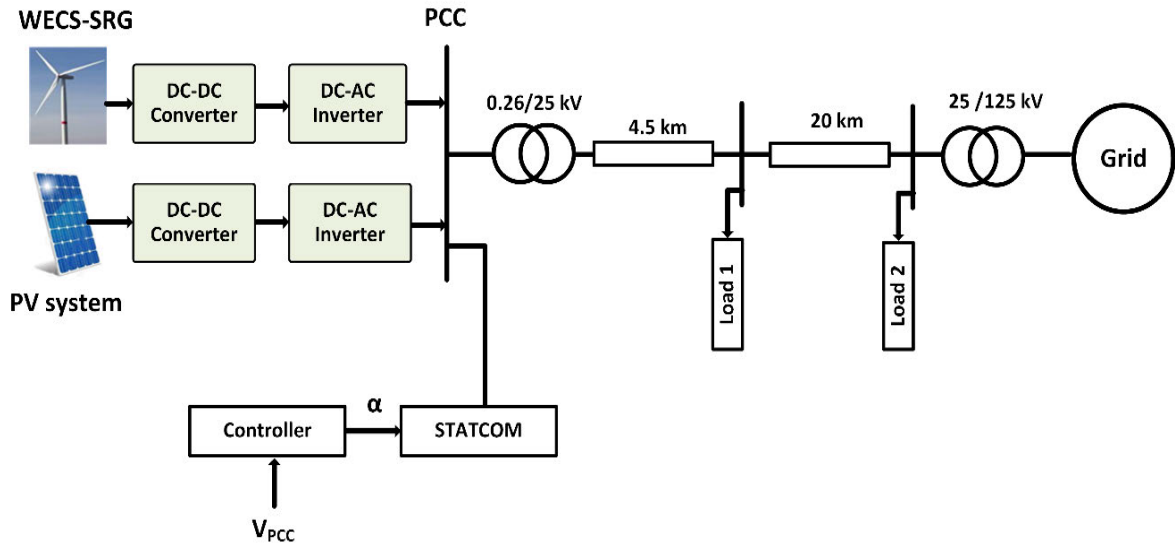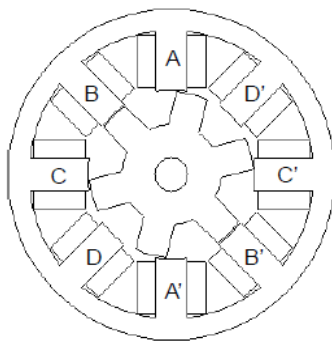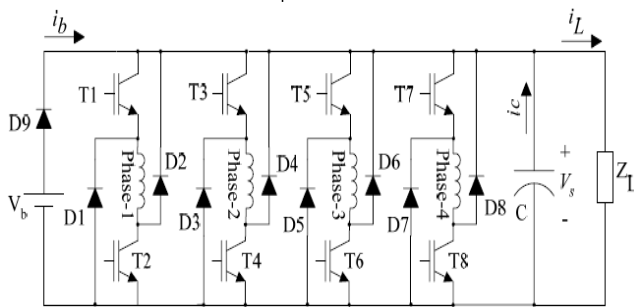**FIGURE 3.** System under investigation.

a- Four-phase 8/6 SRG

b- SRG power converter

FIGURE 4. SRG structure.

phases [33]. The magnetic flux linkage to the windings is determined by integrating the difference between both signals: the input voltage and the voltage drop on the stator resistance Rs [33]:

$$\lambda(t) = \int_0^t (V - i_s R_s) dt \qquad (1)$$

where, both (V and i_s) are the is the (terminal voltage and phase current) respectively.

Then the total torque of the SRG is the summation of torque of all phases;

$$T_e = \sum_{j=1}^{N_s} T_j(\theta, i_s) \qquad (2)$$

The average SRG phases electric power P_{out} is the mean value of the summation of each phase's output power in a single electric cycle.

$$P_{out} = \frac{1}{T_G} \sum_{j=1}^{N_s} \int_0^T v_j i_{s_j} dt \qquad (3)$$

where *Ns* refers to the phases number. T_G denotes to the conduction period of one phase. The (voltage and current) of phase *j* are (V_j and i_j), respectively.

B. PHOTOVOLTAIC SYSTEM
Solar PV systems become gradually important, owing to their compromised benefits compared to other RESs. Some contrasting mathematical models can be used for modeling the PV array. The cell is commonly a wide area p-n diode with a junction near the top surface [35], [36]. Thus, the practical solar cell can be simply modeled by a current source parallel to a diode. This architecture mathematically describes the PV's I-V characteristic.

The PV model equivalent circuit is depicted in Fig. 5, [32], [33]. The PV array output current and voltage are I and V, respectively.

The *I-V* characteristic of the PV cell is expressed as:

$$I_0 = \frac{I_{scn} + K_i \Delta T}{\exp\left(\frac{V_{ocn} + K_v \Delta T}{aV_t}\right) - 1} \qquad (4)$$

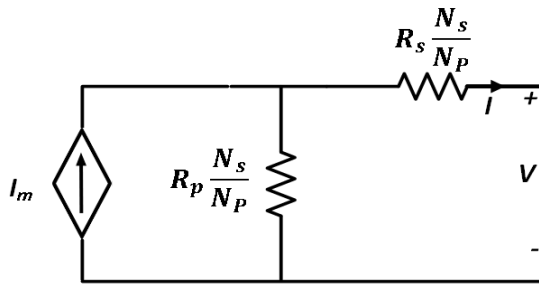$$I_{pv} = (I_{pvn} + K_i \Delta T)\frac{G}{G_n} \qquad (5)$$

FIGURE 5. Equivalent Circuit of PV module.

$$I_m = I_{PV}N_p - I_0 N_p \left[exp\left(\frac{V + R_s \left(\frac{N_s}{N_p} \right) I}{V_t a N_s} \right) - 1 \right] \quad (6)$$

The thermal voltage of the PV array, V_t, is estimated by [32], [33]:

$$V_t = \frac{N_s k T}{q} \quad (7)$$

The KC200GT module is used in this research with a maximum power point tracking (MPPT) approach based on incremental conductance is proposed [35], [36].

C. STATCOM PRINCIPLE OF OPERATION AND CONTROL

STATCOM, the static shunt compensator with capacitive/ inductive output current, can be controlled based on the PCC voltage. The operation principle of STATCOM can be described through STATCOM single line diagram and control block diagram illustrated in Fig.6-a and b, respectively.

STATCOM comprises of a VSC, a DC capacitive energy storage device, and a coupling transformer connecting in shunt the VSC to the power network at PCC. The VSC generates a group of controllable voltages with the AC power system's frequency. STATCOM can operate in capacitive and inductive modes based on the difference between the PCC voltage and the reference voltage assumed to 1pu based on a 0.26 kV base voltage. If the PCC voltage amplitude decreases, a leading current is injected from STATCOM to the grid at PCC, i.e. the STATCOM generates reactive power (capacitive mode). While in the inductive mode, a lagging current is injected from STATCOM to the grid at PCC. Thus, the STAT-COM absorbs the reactive power when the PCC increases. If the PCC voltage is not changed, no power exchange takes place. This controllable injected current from STATCOM suppress the PCC voltage fluctuations during fault events. This work's major contribution is the near-optimal scheduling of two PI controllers to efficiently drive the STATCOM to suppress the voltage fluctuations and consequently improve the hybrid system dynamic performance. Scheduling the parameters of the two PI controllers is performed by WOA. WOA is used for minimizing the integral of the square of error (ISE). Such error is the difference between the reference and the PCC voltages. The STATCOM block diagram and the two optimized PI controllers, depicted in Fig. 6-b, show the

a.   Single-phase diagram of STATCOM
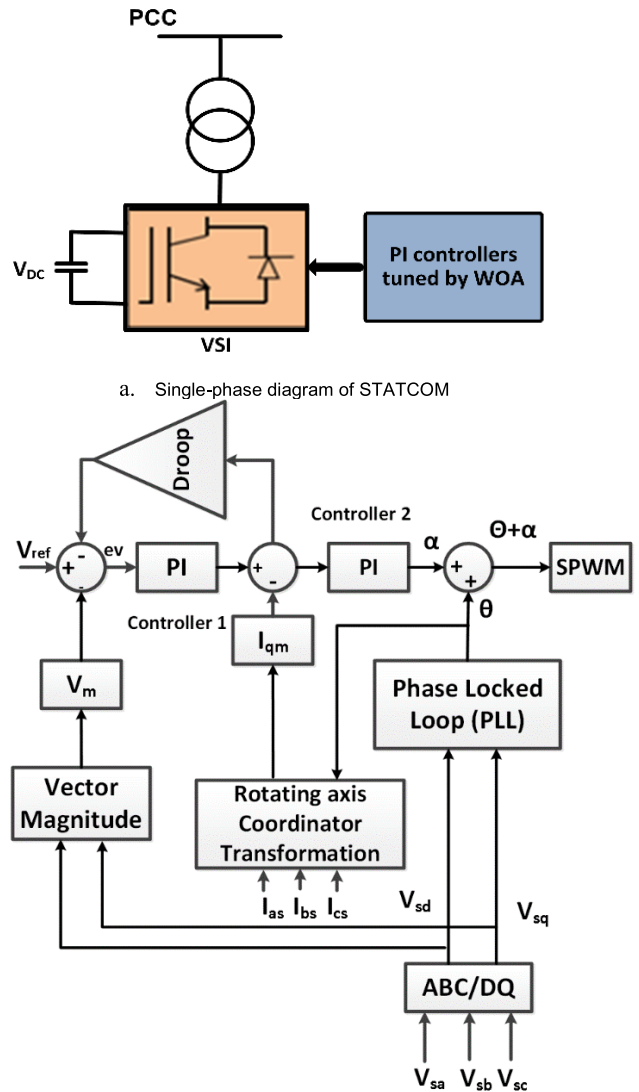
b.   Block diagram of PI-STATCOM controller

FIGURE 6. STATCOM circuit representation.

d-q frame transformation of the three-phase PCC signals of both voltages and currents. The two proposed controllers are mainly used for driving the STATCOM. Controller 1 is considered to provide the due updates to the quadrature-axis current reference, Iq_{ref}, according to the difference between both measured and reference voltage signals. Controller 2 is principally for driving the angle α added to the phase angle of the PCC's terminal voltage denoted $\ominus$. In this paper, the SPWM technique is introduced to generate switching pulses of the STATCO's three-level inverter. Therefore, the inverter voltage supplied to the grid is regulated in accordance with the phase angle α control [22].

The major contribution of this paper is proposing the WOA for determining the near-optimal PI controller parameters for STATCOM. PSO, an alternative optimization technique, is used for providing an impartial comparative analysis

regarding the system dynamic performance when controlled with the optimized two PI controllers.

D. PARTICLE SWARM FOR TUNING PI CONTROL PARAMETERS

PSO is mainly considered for determining the near-optimal PI control parameters to control reactive power flow between the hybrid system and the STATCOM-based grid. As demonstrated in Fig. 6-b, two different PI controllers are assigned to drive the STATCOM. Each PI controller has its own two gains (K_p, K_I). The optimization process using PSO is introduced to determine the optimal PI controllers parameters while minimizing J's objective function during any fault events.

The objective function, *J*, can be defined as:

$$J = \int_0^t \left(ev(t)^2 \right) dt \qquad (8)$$

Initial pollution for the two controller's parameters is assumed and the objective function is calculated based on these initial values. Both the velocity/position of each particle are updated. Accordingly, the new objective function is defined. With continuous updates, such a process is repeated till reaching either the maximum number of iteration or the near-optimal solution. Finally, the best population leading to the minimum objective function is estimated. The PSO flowchart for optimal tuning of tuning the two PI controller's parameters is depicted in Fig. 7 [37].

E. WALE OPTIMIZATION ALGORITHM FOR TUNING PI CONTROL PARAMETERS

WOA, a recent optimization technique, mimics the whale behavior as it is among the most intelligent animals. Some of their brain cells are common to human cells [33]. By applying such WOA, the solution starts by assuming random solutions for the optimized four parameters of both PI controllers and the corresponding objective function J, introduced in (8) is determined. In WOA, search agents updates are performed each iteration position, and the objective function is determined accordingly. The process is repeated till attaining the maximum number of iterations and the best solution is stored. The flow chart of WOA for optimal tuning of PI control parameters is given in Fig. 8.

The optimization process based WOA can be divided into three steps:

1) SURROUNDING PREY WHALES

The humpback whales initially perceive the location; then circle the prey. The calculation of WOA forecasts the present best solution as the solution close to the best one. After characterizing the best solution, other search whales (operators) update their individual positions for reaching the best arrangement. The mathematical presentation corresponds to the whales surrounding prey methodology can be expressed as [30]:

$$\overrightarrow{H} = \left| \overrightarrow{E}.\overrightarrow{Y^P}(i) - \overrightarrow{Y}(i) \right| \qquad (9)$$
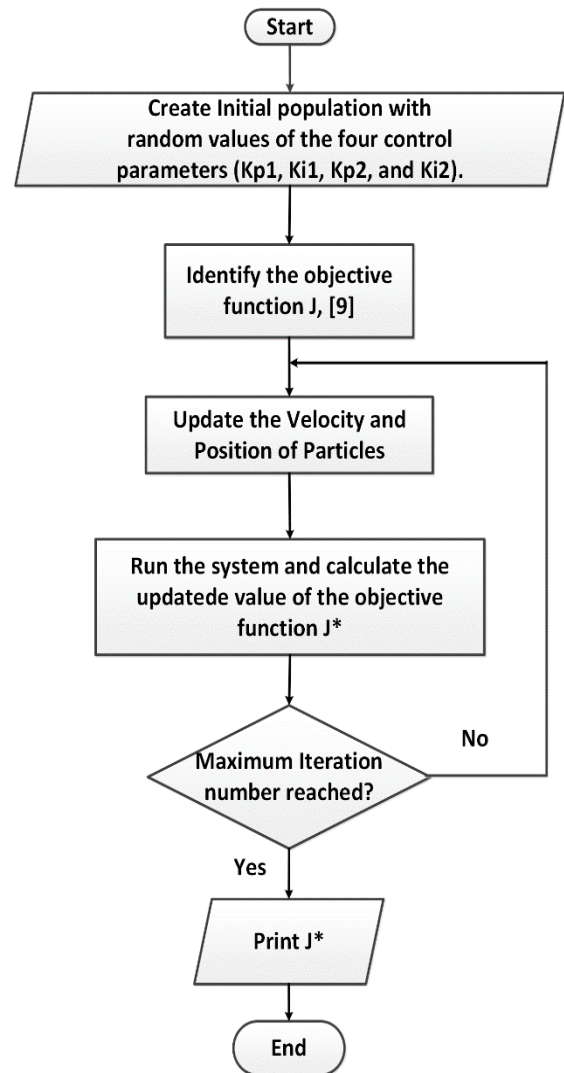
FIGURE 7. Flow Chart of optimal tuning PI controller's parameters using PSO.

$$\overrightarrow{Y}(i+1) = \overrightarrow{Y^P}(i) - \overrightarrow{D}.\overrightarrow{H} \qquad (10)$$

where *i* refers to the current iteration.

Both vector coefficients D and $\overrightarrow{E}$ are determined as:

$$\overrightarrow{E} = 2r_2 \qquad (11)$$
$$\overrightarrow{D} = 2\overrightarrow{d}.r_1 - \overrightarrow{d} \qquad (12)$$

The value of D decreases from 2 to 0, the vector $\overrightarrow{D}$ ranges from $\left[-\overrightarrow{d}, \overrightarrow{d} \right]$. The random values ($r_1$ and r_2) are between 0 and 1.

2) ASSAULTING INSTRUMENT OF THE WOA (BUBBLE-NET CHASING)/EXPLOITATION STAGE

In this bubble-net chasing step, two methodologies are defined, shrinking encircling mechanism and spiral updating position. The whales' shrinking attitude is performed by reducing the value of $\overrightarrow{d}$. While the second methodology is
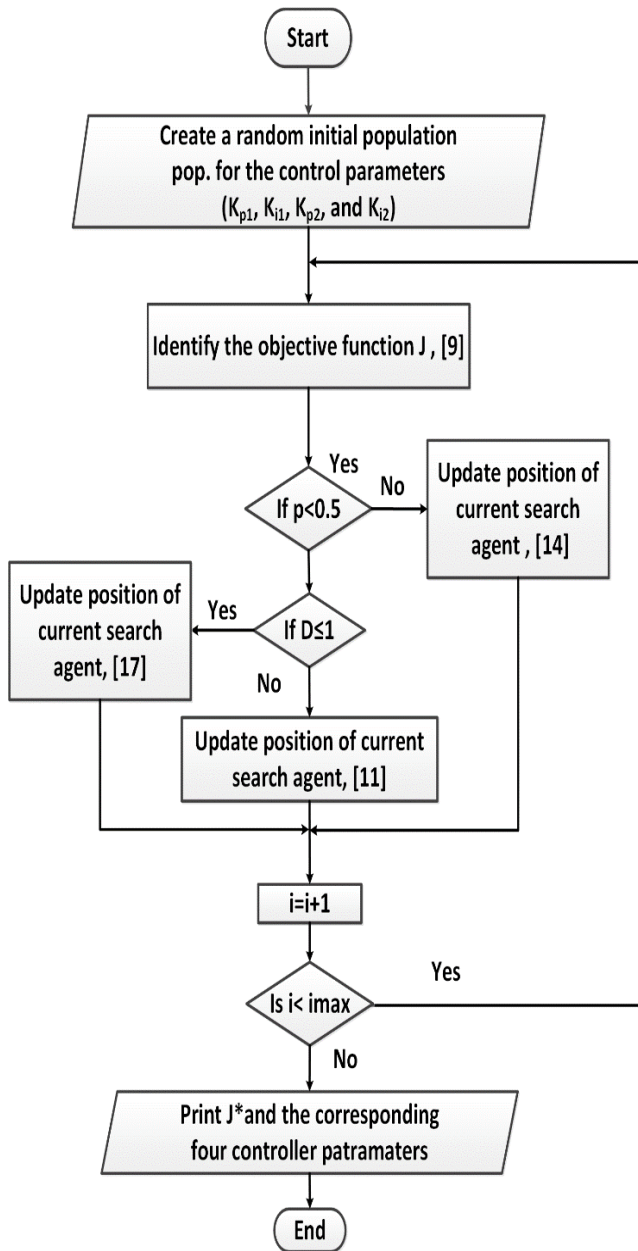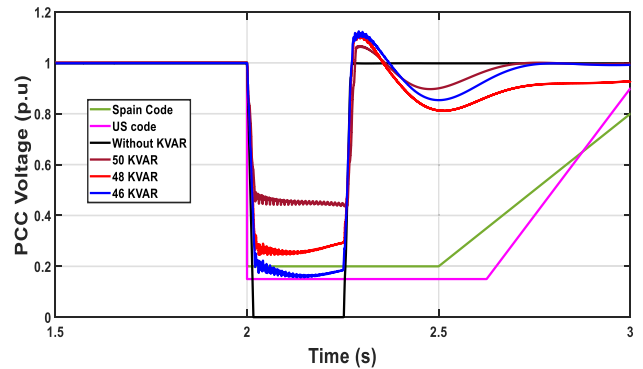
FIGURE 9. Voltage at PCC with different kVAR compensation.

3) PREY SEARCHING STEP

The searching step principally relies on the fluctuation of the vector. Regarding each other position, the best position is randomly searched for by humpback whales search. For reaching an optimal global position, (15) and (16) are followed:

$$\overrightarrow{F} = \left| \overrightarrow{D}.\overrightarrow{Y^{rand}} - \overrightarrow{Y} \right| \quad (15)$$

$$\overrightarrow{Y}(i+1) = \overrightarrow{Y^{rand}} - \overrightarrow{D}.\overrightarrow{H} \quad (16)$$

where Y^{rand}, is a random whale position vector selected from the current population.

IV. RESULTS AND DISCUSSIONS

The MATLAB/SIMULINK^{TM} is used for simulating the hybrid model integrated into the grid and the STATCOM. The WOA and PSO are used for the near-optimal scheduling of the two PI controller parameters for driving the STATCOM. Therefore, the overall system dynamic performance is enhanced during any abnormal operating conditions, including the PCC's undesired three-phase faults.

A. STATCOM SIZING

There are various criteria for determining the appropriate size of STATCOM [22], [38], [39]. In this study, the amount of reactive power needed from compensation is assumed to be equal to the sum of WECS and PV systems' ratings. A three-phase fault is applied at the PCC, and the PCC voltage is measured. By gradually decreasing the reactive power to its minimum value at which the PCC voltage level still ranges in the continuous operating zones.

A three-phase to ground fault is simulated at PCC between 2 and 2.25s with injected reactive power of 124.8 kVA. The minimum reactive power that could be injected during this fault and the PCC voltage is still in the continuous operating zone is 48 kVAR, as shown in Fig. 9.

B. THREE-PHASE FAULT

In this case study, the three-phase to ground fault is employed at the PCC between 2 and 2.25s. Both PSO and WOA are used for determining the near-optimal PI controller of the

based on updating the position attitude and can be defined as [30]:

$$\overrightarrow{Y}(i+1) = \overrightarrow{F'}.b_{el}(2\pi r) + \overrightarrow{Y^P}(i) \quad (13)$$

During chasing, whales use to swim near around the prey in the previous two strategies at the same time. To update the whales' positions, 50% probability is considered for these two strategies as [30]:

$$\overrightarrow{Y}(it+1) = \begin{cases} \overrightarrow{Y^P}(i) - \overrightarrow{D}.\overrightarrow{H} & p < 0.5 \\ \overrightarrow{F'}.b_{el}(2\pi r) + \overrightarrow{Y^P}(i) & p \geq 0.5 \end{cases} \quad (14)$$

STATCOM. The size of the STATCOM is 48 kVA. The convergence of the objective function, J introduced in (8) when using PSO and WOA is indicated in Fig. 10.
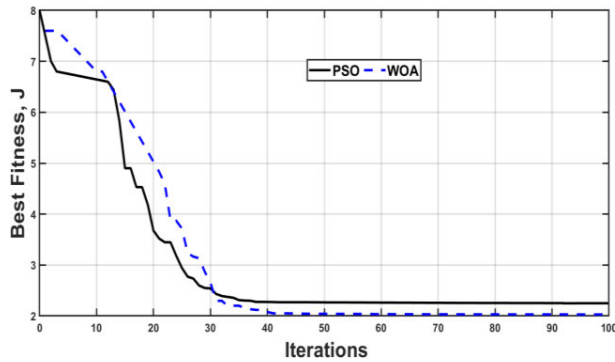

FIGURE 10. Convergence of the objective function using PSO and WOA.

The PI controllers parameters using PSO and WOA are given in Table 2, while the three-phase fault to ground is applied to the system at PCC between 2 and 2.25s.

TABLE 2. Control parameters using PSO and WOA.

	PSO		WOA	
	Controller 1	Controller 2	Controller 1	Controller 2
Kp	9.76	15.7	12.6	20.8
Ki	3.8	9.6	14.8	16.2

The PCC voltage with and without STATCOM is depicted in Fig.11-a. Without STATCOM, the PCC voltage ranges out of the continuous operating zone (for both Spain and US codes) that will call the RES, including WECS and PV to be disconnected from the grid. The reconnection of these RES to the grid is not an easy issue, as it requires some complicated steps and procedures. Adding the controlled STATCOM to the system had improved the PCC voltage profile with the superiority of using WOA-PI than PSO-PI. The PCC voltage reaches 0.35 and 0.4 pu when using PSO-PI and WOA-PI, respectively. Adding the proposed controlled STATCOM to the system at PCC will the RES in service during the three-phase fault as the PCC voltage ranges within the continuous operating zone. Consequently, WECS and PV system will be in service during this fault event.

Without using STATCOM, the PCC current increased by 1.1 KA with a 320% increase that calls the protection devices to disconnect the interconnection between the RES and the grid. When using the STATCOM, the RES will not be disconnected from the grid due to a slight increase in the PCC current to 0.5 and 0.4551 KA when using PSO-PI and WOA-PI respectively, Fig.11-b. Without adding STATCOM to the system, the SRG power profile is significantly affected by this fault and the power from the SRG increases to higher levels that will disconnect the generator from the network. By adding STSTCOM to the system, the SRG profile is
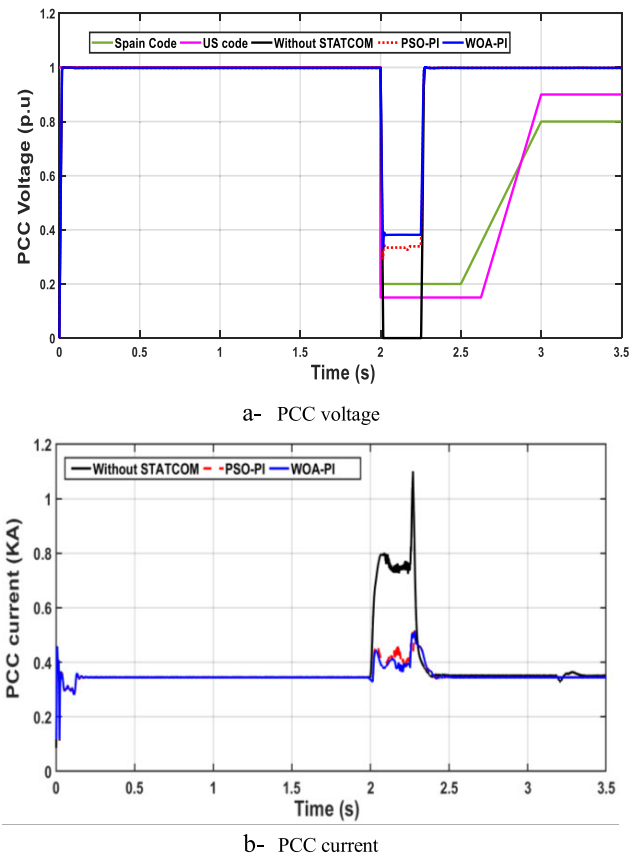

a- PCC voltage

b- PCC current

FIGURE 11. PCC voltage and current with and without STATCOM.

improved and ranges in the acceptable limits that will keep the generator in service as in Fig.11-c.

The WECS performance through the SRG in this three-phase fault will be investigated. The SRG's DC voltage increased to 480 V and this voltage cannot return to the steady-state value of 230V without using STATCOM after clearing the fault at 2.25s. When the controlled STATCOM proposed was connected to the PCC, the SRG DC voltage profile is improved and the DC voltage can come back to the steady-state value as in Fig.12-a. If the SRG remains grid-connected, any undesired increase in the DC voltage results in undesired damage of the DC link. The same scenario is illustrated for the SRG current as in Fig.12-b. The SRG current reached to a steady-state value of 151A rather than 111 when using STATCOM. These results and discussions emphasize the disconnection of the WECS from the grid as investigated from the PCC voltage profile and the grid codes as in Fig.9-a. The protection devices will disconnect the SRG as the high current drawn from the SRG during this fault event. The SRG output power increases and can not retain to its steady-state value before fault without using STATCOM. Consequently, the application of the STATCOM enables maintaining the SRG output power range in the acceptable limits and could retain its steady-state value before fault as shown in Fig.12-c.

The PV system dynamic performance is depicted in Fig. 13. The PV system is slightly influenced by the
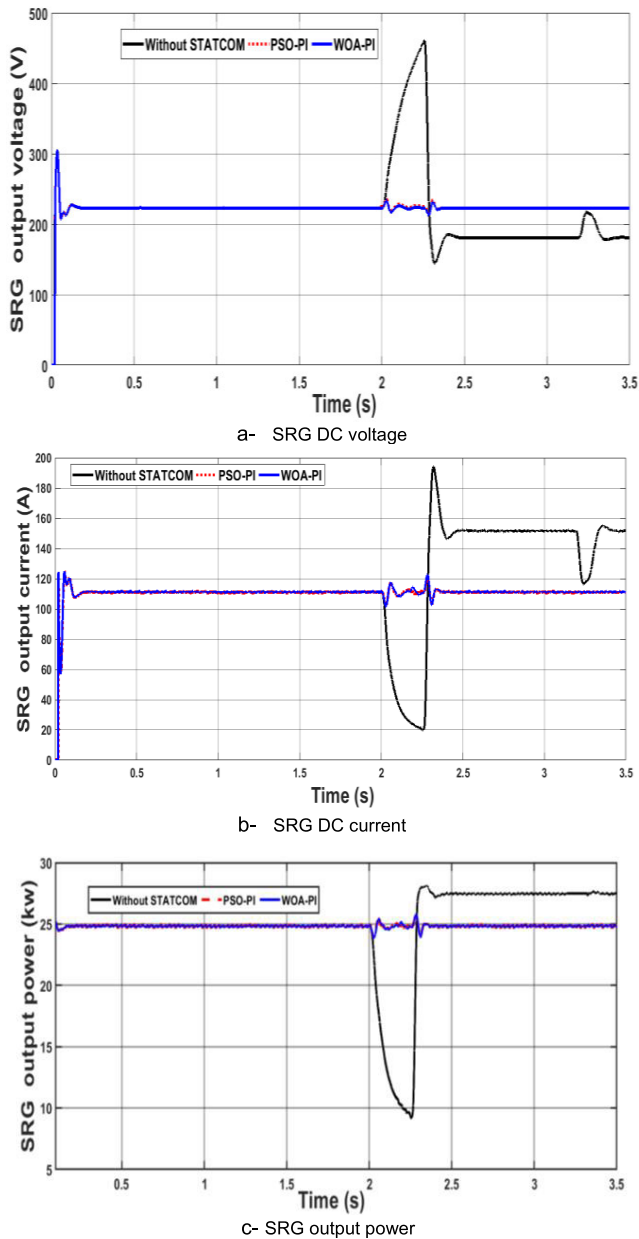
a-   SRG DC voltage

b-   SRG DC current

c- SRG output power

FIGURE 12. SRG performance.

a-   PV DC voltage

b-   PV DC current

FIGURE 13. PV performance.

FIGURE 14. STATCOM reactive power during three-phase fault using PSO and WOA.

FIGURE 15. Wind gust.

three-phase fault at the PCC while considering the MPPT for PV system.

During normal operation before conditions, no exchange of reactive power between the STATCOM and the system. During this severe fault, the role of the STATCOM is to act as a static VAR compensator to regulate the PCC voltage shown in Fig.14.

C. WIND GUST
Wind gust, as a disturbance, is applied to the system. Wind gust events will affect both the voltage profile at the PCC and the SRG voltage. The wind gust is simulated in this study by random changes of the wind speed applied to the WECS between 8 and 15 m/s, as shown in Fig. 15.
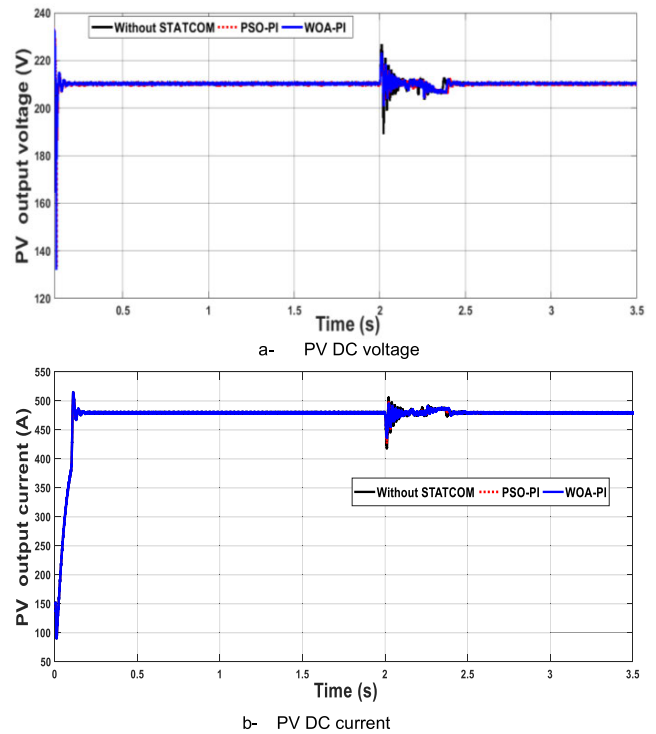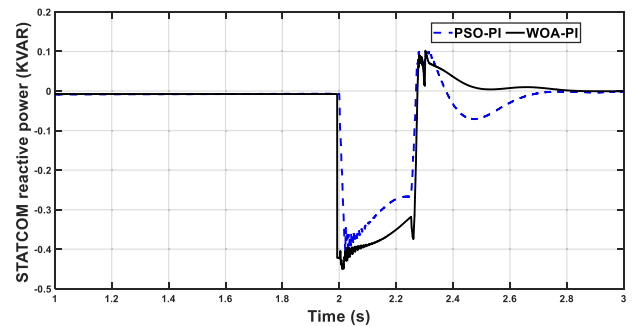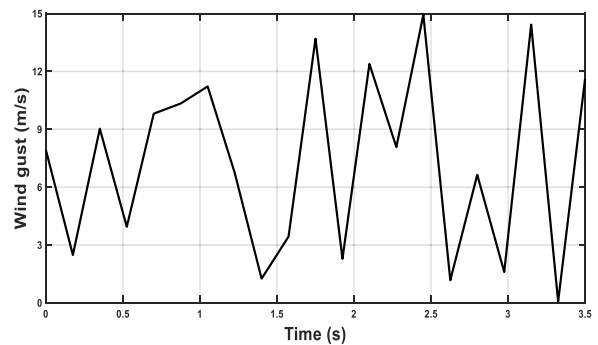
Due to this wind gust, the SRG voltage and the PCC voltage oscillate around the rated value with more harmonics and distortions without using STATCOM. Connecting the controller
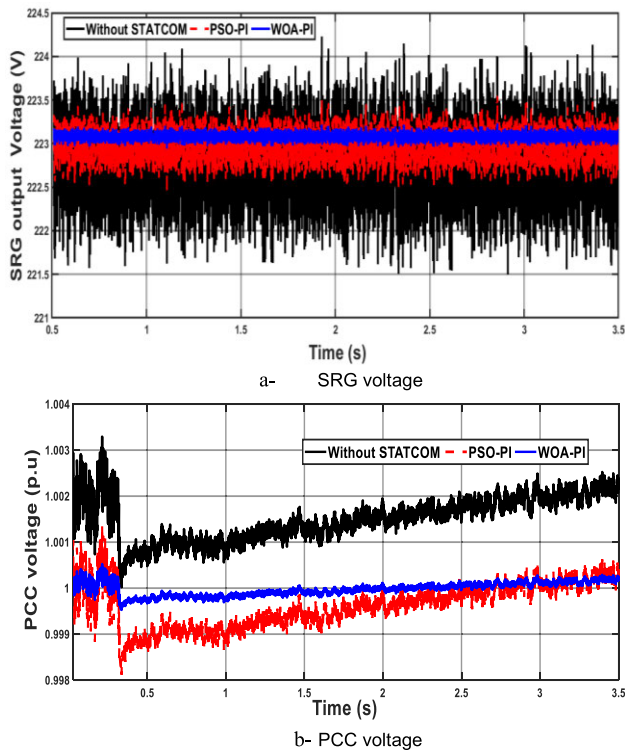
FIGURE 16. **WECS performance during wind gust.**

STATCOM to the system, the SRG and PCC voltages are improved, and the WOA surplus PSO, Fig.16 a and b.

V. CONCLUSION AND PERSPECTIVES

The use of STATCOMs to enhance the dynamic performance of non-linear renewable-based hybrid systems, including WECS and PVs in the presence of wind gusts and guaranteeing the system's efficient continuous operation of RESs during faults are a real challenge. The reactive power flow between the STATCOM and the hybrid system is governed and the voltage is regulated at PCC through the near-optimal scheduling of two PI controllers using metaheuristic optimizers, WOA and PSO, respectively. From the numerical simulations, the WOA, as a novel optimization technique, is considered an ideal metaheuristic optimizer for the near-optimal gain scheduling of the STATCOM PI control parameters. In comparison with the PSO, employing the WOA to control the STATCOM enables the system's reactive power during wind gusts and fault events. Consequently, the proper control of the STATCOM efficiently results in (i) enhancing the dynamic performance of the hybrid grid-connected power system consists of WECS and PV system; (ii) increasing the system's FRT capability while keeping the RES grid-connected during undesired abnormal operating conditions without disconnection.

Through the impartial quantitative and qualitative comparison between the STATCOM-PI controllers optimized by WOA and PSO, WOA shows better dynamic performance than PSO.

APPENDIX
SRG parameters

	$\alpha=1^\circ$, $\beta=16$
DC bus o/p Voltage V_o	230 V
DC bus o/p Current I_{dc}	99.2 A
Output power P_{out}	24.8 kW

KC200GT module parameters

Quantity	Value
I max power	7.61 A
V max power	26.3 V
P max	200.143 W
I short circuit	8.21 A
V open circuit	32.9 V
I leakage	$9.825*10^{-8}$ A
I photovoltaic	8.211 A
Diode ideality constant (a)	1.3
Parallel resistance	415.406 Ω
Series resistance	0.221 Ω

STATCOM data

rating	48 kVA
Series line resistance	0.34 Ω
Series line reactance	3.63 Ω
DC- link capacitance	250μF

REFERENCES
[1] S. Liaquat, M. S. Fakhar, S. A. R. Kashif, A. Rasool, O. Saleem, and S. Padmanaban, "Performance analysis of APSO and firefly algorithm for short term optimal scheduling of multi-generation hybrid energy system," *IEEE Access*, vol. 8, pp. 177549–177569, 2020.

[2] G. S. Chawda, A. G. Shaik, M. Shaik, S. Padmanaban, J. B. Holm-Nielsen, O. P. Mahela, and P. Kaliannan, "Comprehensive review on detection and classification of power quality disturbances in utility grid with renewable energy penetration," *IEEE Access*, vol. 8, pp. 146807–146830, 2020.

[3] W. S. Hassanein, M. M. Ahmed, M. O. A. El-Raouf, M. G. Ashmawy, and M. I. Mosaad, "Performance improvement of off-grid hybrid renewable energy system using dynamic voltage restorer," *Alexandria Eng. J.*, vol. 59, no. 3, pp. 1567–1581, 2020.

[4] M. M. Samy, M. I. Mosaad, and S. Barakat, "Optimal economic study of hybrid PV-wind-fuel cell system integrated to unreliable electric utility using hybrid search optimization technique," *Int. J. Hydrogen Energy*, Sep. 2020, doi: 10.1016/j.ijhydene.2020.07.258.

[5] H. Bahrampour, A. K. B. Marnani, M. B. Askari, and M. R. Bahrampour, "Evaluation of renewable energies production potential in the middle east: Confronting the world's energy crisis," *Frontiers Energy*, vol. 14, no. 1, pp. 42–56, Mar. 2020.

[6] "Nordisk regelsamling (nordic grid code)," Nordel Corp., Tech. Rep., 2004.

[7] M. I. Mosaad and F. Salem, "Adaptive voltage regulation of self excited induction generator using FACTS controllers," *Int. J. Ind. Electron. Drives*, vol. 1, no. 4, p. 219, 2014.

[8] M. I. Mosaad, A. Alenany, and A. Abu-Siada, "Enhancing the performance of wind energy conversion systems using unified power flow controller," *IET Gener., Transmiss. Distrib.*, vol. 14, no. 10, pp. 1922–1929, May 2020.

[9] M. I. Mosaad, "Direct power control of SRG-based WECSs using optimised fractional-order PI controller," *IET Electric Power Appl.*, vol. 14, no. 3, pp. 409–417, Mar. 2020.

[10] N. G. Hingorani, "Flexible AC transmission," *IEEE Spectr.*, vol. 30, no. 4, pp. 40–45, Apr. 1993, doi: 10.1109/6.206621.

[11] A. M. Othman and A. A. El-Fergany, "Design of robust model predictive controllers for frequency and voltage loops of interconnected power systems including wind farm and energy storage system," *IET Gener., Transmiss. Distrib.*, vol. 12, no. 19, pp. 4276–4283, Oct. 2018.

[12] M. I. Mosaad *et al.*, "Optimal PI controller of DVR to enhance the performance of hybrid power system feeding a remote area in Egypt," *Sustain. Cities Soc.*, vol. 47, pp. 101469–101483, 2019.

[13] R. Fadaeinedjad, G. Moschopoulos, and M. Moallem, "Using STATCOM to mitigate voltage fluctuations due to aerodynamic aspects of wind turbines," in *Proc. IEEE Power Electron. Specialists Conf.*, Jun. 2008, pp. 3648–3654.

[14] M. I. Mosaad, A. Abu-Siada, and M. F. El-Naggar, "Application of superconductors to improve the performance of DFIG-based WECS," *IEEE Access*, vol. 7, no. 1, pp. 103760–103769, Dec. 2019.

[15] Y. M. Alharbi, A. M. S. Yunus, and A. A. Siada, "Application of UPFC to improve the LVRT capability of wind turbine generator," in *Proc. 22nd Austral. Universities Power Eng. Conf. (AUPEC)*, 2012, pp. 1–4.

[16] H. Sebaa, K. R. Guerriche, and T. Bouktir, "Optimal sizing and placement of renewable energy source in large scale power system using ABC technique in presence of UPFC," in *Proc. Int. Renew. Sustain. Energy Conf. (IRSEC)*, Ouarzazate, Morocco, Oct. 2014, pp. 294–299, doi: 10.1109/IRSEC.2014.7059912.

[17] E. M. Molla and C.-C. Kuo, "Voltage sag enhancement of grid connected hybrid PV-wind power system using battery and SMES based dynamic voltage restorer," *IEEE Access*, vol. 8, pp. 130003–130013, 2020, doi: 10.1109/ACCESS.2020.3009420.

[18] L. Yan, X. Chen, X. Zhou, H. Sun, and L. Jiang, "Perturbation compensation-based non-linear adaptive control of ESS-DVR for the LVRT capability improvement of wind farms," *IET Renew. Power Gener.*, vol. 12, no. 13, pp. 1500–1507, Oct. 2018, doi: 10.1049/iet-rpg.2017.0839.

[19] S. Wang, S. Chen, L. Ge, and L. Wu, "Distributed generation hosting capacity evaluation for distribution systems considering the robust optimal operation of OLTC and SVC," *IEEE Trans. Sustain. Energy*, vol. 7, no. 3, pp. 1111–1123, Jul. 2016, doi: 10.1109/TSTE.2016.2529627.

[20] M. A. E. Zaki *et al.*, "Power quality improvement of WEGCS using STATCOM based EC techniques," *Int. J. Ind. Electron. Drives*, vol. 3, no. 4, pp. 229–237, 2017.

[21] H. Kuang, L. Zheng, S. Li, and X. Ding, "Voltage stability improvement of wind power grid-connected system using TCSC-STATCOM control," *IET Renew. Power Gener.*, vol. 13, no. 2, pp. 215–219, Feb. 2019, doi: 10.1049/iet-rpg.2018.5492.

[22] M. I. Mosaad, "Model reference adaptive control of STATCOM for grid integration of wind energy systems," *IET Electr. Power Appl.*, vol. 12, no. 5, pp. 605–613, May 2018.

[23] K. Sarita, S. Kumar, A. S. S. Vardhan, R. M. Elavarasan, R. K. Saket, G. M. Shafiullah, and E. Hossain, "Power enhancement with grid stabilization of renewable energy-based generation system using UPQC-FLC-EVA technique," *IEEE Access*, vol. 8, pp. 207443–207464, 2020, doi: 10.1109/ACCESS.2020.3038313.

[24] M. I. Mosaad and H. S. Ramadan, "Power quality enhancement of grid-connected fuel cell using evolutionary computing techniques," *Int. J. Hydrogen Energy*, vol. 43, no. 25, pp. 11568–11582, Jun. 2018.

[25] R. Chedid and S. Rahman, "Unit sizing and control of hybrid wind-solar power systems," *IEEE Trans. Energy Convers.*, vol. 12, no. 1, pp. 79–85, Mar. 1997, doi: 10.1109/60.577284.

[26] N. D. Galan, J. R. Rosas, J. L. Rios, J. M. Canedo, and A. Loukianov, "Application of PI and super twisting drivers to voltage regulation of wind farm via StatCom," *IEEE Latin Amer. Trans.*, vol. 13, no. 2, pp. 462–468, Feb. 2015, doi: 10.1109/TLA.2015.7055565.

[27] M. Wang, X. Wang, J. Qiao, and L. Wang, "Improved current decoupling method for robustness improvement of LCL-type STATCOM based on active disturbance rejection control," *IEEE Access*, vol. 7, pp. 121781–121792, 2019, doi: 10.1109/ACCESS.2019.2931747.

[28] O. M. Kamel, A. A. Z. Diab, T. D. Do, and M. A. Mossa, "A novel hybrid ant colony-particle swarm optimization techniques based tuning STATCOM for grid code compliance," *IEEE Access*, vol. 8, pp. 41566–41587, 2020, doi: 10.1109/ACCESS.2020.2976828.

[29] J.-H. Park and Y.-K. Choi, "An on-line PID control scheme for unknown nonlinear dynamic systems using evolution strategy," in *Proc. IEEE Int. Conf. Evol. Comput.*, May 1996, pp. 759–763.

[30] P. R. Sahu, P. K. Hota, and S. Panda, "Modified whale optimization algorithm for fractional-order multi-input SSSC-based controller design," *Optim. Control Appl. Methods*, vol. 39, no. 5, pp. 1802–1817, Jun. 2018.

[31] N. K. Saxena and A. Kumar, "Reactive power control in decentralized hybrid power system with STATCOM using GA, ANN and ANFIS methods," *Int. J. Electr. Power Energy Syst.*, vol. 83, pp. 175–187, Dec. 2016, doi: 10.1016/j.ijepes.2016.04.009.

[32] N. Saxena and A. Kumar, "Reactive power compensation of an isolated hybrid power system with load interaction using ANFIS tuned STATCOM," *Frontiers Energy*, vol. 8, no. 2, pp. 261–268, Jun. 2014, doi: 10.1007/s11708-014-0298-6.

[33] H. Le-Huy, "Performance study of a four-phase 8/6 switched reluctance generator using a nonlinear model based on magnetization curves," in *Proc. 35th Annu. Conf. IEEE Ind. Electron.*, Nov. 2009, pp. 3910–3915.

[34] M. I. Mosaad, N. I. Elkalashy, and M. G. Ashmawy, "Integrating adaptive control of renewable distributed switched reluctance generation and feeder protection coordination," *Electr. Power Syst. Res.*, vol. 154, pp. 452–462, Jan. 2018.

[35] M. G. Villalva, J. R. Gazoli, and E. R. Filho, "Modeling and circuit-based simulation of photovoltaic arrays," *Eletrônica de Potência*, vol. 14, no. 1, pp. 35–45, Feb. 2009.

[36] M. O. A. El-Raouf, M. I. Mosaad, A. Mallawany, M. A. Al-Ahmar, and F. M. El Bendary, "MPPT of PV-wind-fuel cell of off-grid hybrid system for a new community," in *Proc. 20th Int. Middle East Power Syst. Conf. (MEPCON)*, 2018, pp. 480–487.

[37] H. Chen, J. Li, and X. Zhou, "PSO-based self-tuning PI control for STATCOM," in *Proc. 7th Int. Power Electron. Motion Control Conf. (IPEMC)*, no. 4, Jun. 2012, pp. 2710–2715.

[38] B. Singh, S. S. Murthy, and S. Gupta, "Analysis and design of STATCOM-based voltage regulator for self-excited induction generators," *IEEE Trans. Energy Convers.*, vol. 19, no. 4, pp. 783–790, Dec. 2004.

[39] Y. K. Gounder, D. Nanjundappan, and V. Boominathan, "Enhancement of transient stability of distribution system with SCIG and DFIG based wind farms using STATCOM," *IET Renew. Power Gener.*, vol. 10, no. 8, pp. 1171–1180, Sep. 2016.

MOHAMED I. MOSAAD received the B.Sc. and M.Sc. degrees from Zagazig University, Egypt, and the Ph.D. degree from Cairo University, Egypt, all in electrical engineering. He is currently an Associate Professor with the Department of Electrical and Electronic Engineering Technology, YIC, KSA, author of more than 70 high-ranked journal and conference papers. His research interests include power system stability, control, optimization, and renewable energy. He is the editor-In Chief for YJES. He is a reviewer for the IEEE TRANSACTION ON POWER DELIVERY, IEEE TRANSACTION ON ENERGY CONVERSION, *IET Electric Power Application Journal, IET Generation Transmission and Distribution Journal, IET Journal of Engineering, IET System Integration, Journal of Cleaner Production, Electric Power System Components, International Journal of Industrial Electronics and Drives (IJIED)*, IEEE ACCESS JOURNAL, *Electric Power System Research, Energies, Alexandria Journal of Engineering, Ain Shams Journal of Engineering, Asian Journal of Control, and International Journal of Energy Engineering* (IJEE).

HAITHAM SAAD MOHAMED RAMADAN received the Ph.D. degree from the Department of Energy and Automatic Control, École Supérieure d'Électricité (SUPELEC), University of South Paris XI, France, in March 2012. In June 2012, he became a Lecturer with the Electrical Power and Machines Department, Faculty of Engineering, Zagazig University, Egypt. Since August 2013, he did several postdoctoral research missions in the Laboratory of Signal and Systems (LSS), the Federation of Research of Fuel Cells (FCLAB), the FEMTO-ST laboratory, and the University of Belfort Montbéliard, France. Since June 2017, he has been an Associate Professor with the Power and Machines Department, Faculty of Engineering, Zagazig University. In 2021, he joined the International Institute ISTHY, l'Institut international sur le Stockage de l'Hydrogène, France. He is the author of more than 80 high-ranked journal and conference papers and one book chapter. His fields of interests include hydrogen reservoirs and hydrogen storage systems, power systems control and optimization, multi-physical modelling of energy systems, renewable energy (Solar and Wind), hybrid power systems, hydrogen economy, hydrogen technologies, fuel cells and batteries, energy management topics, electric and hybrid electric vehicles, microgrids, smart grids, and HVDC. He was/is the Principal Investigator and Coordinator of different Egyptian-French projects and international collaborations; and summer schools. Since 2017, he has been the Co-Chair of the annual International Conference of Emerging and Renewable Energy: Generation and Application (ICEREGA): ICEREGA'20, ICEREGA'19, ICEREGA'18, and ICEREGA'17, the General Secretary of ICREGA16, and the International Program Committee member of ICAFE'17. He is/was the Guest and Managing Editor for different Elsevier journals.

MANSOUR ALJOHANI was born in Jeddah, KSA, in May 1986. He received the B.Sc. degree from the Riyadh College of Technology, KSA, and the M.Sc. and Ph.D. degrees from the University of Dayton, USA, all in electrical engineering. He is currently an Assistant Professor with the Department of Electrical and Electronic Engineering Technology, Yanbu Industrial College (YIC), KSA. His research interests include control systems and signals, power system stability, and renewable energy.

MOHAMED F. EL-NAGGAR was born in Helwan, Egypt, in September 1972. He received the B.Sc. and M.Sc. degrees in electrical engineering from Helwan University, Cairo, in 1995 and 2002, respectively. He received the Ph.D. from Helwan University, Egypt, in 2009. He is a Teacher of power system protection, Power and Machines Engineering Dept., Faculty of Engineering, Helwan University, Cairo, Egypt. His research interests include power system relaying.

SHERIF S. M. GHONEIM (Senior Member, IEEE) received the B.Sc. and M.Sc. degrees from the Faculty of Engineering, Shoubra, Zagazig University, Egypt, in 1994 and 2000, respectively, and the Ph.D. degree in electrical power and machines from the Faculty of Engineering, Cairo University, in 2008. Since 1996, he has been teaching at the Faculty of Industrial Education, Suez Canal University, Egypt. From the end of 2005 to the end of 2007, he was a Guest Researcher at the Institute of Energy Transport and Storage (ETS) of the University of Duisburg–Essen in Germany. He joined Taif University as an Associate Professor with the Electrical Engineering Department, Faculty of Engineering. His research areas include grounding systems, dissolved gas analysis, breakdown in SF_6 gas, and AI technique applications.

• • •